Nanoscale

Self-scrolling MoS2 Metallic Wires

Journal:	*Nanoscale*
Manuscript ID	NR-ART-06-2018-004611.R1
Article Type:	Paper
Date Submitted by the Author:	15-Aug-2018
Complete List of Authors:	Wang, Zegao; Aarhus University, Interdisciplinary Nanoscience Center (iNANO) Wu, Hong-Hui; University of Nebraska–Lincoln , Department of Chemistry Li, Qiang; Key Laboratory for Colloid and Interface Chemistry, Shandong University Besenbacher, Flemming; Aarhus University, Interdisciplinary Nanoscience Center Zeng, Xiao; University of Nebraska-Lincoln, Chemistry Dong, Mingdong; Aarhus University, Interdisciplinary Nanoscience Center (iNANO)

Journal Name

ARTICLE

Self-scrolling MoS_2 Metallic Wires

Zegao Wang,‡[ab] Hong-Hui Wu,‡[c] Qiang Li,[bd] Flemming Besenbacher,[b] Xiao Cheng Zeng*[ce] and Mingdong Dong*[b]

Received 00th January 20xx,
Accepted 00th January 20xx

DOI: 10.1039/x0xx00000x

www.rsc.org/

Two dimensional (2D) van der Waals (vdW) materials with strong in-plane chemical bonds and weak interaction in the out-of-plane direction have been acknowledged as a basic building block for designing dimensional materials in 0D, 1D, 2D and 3D forms. Compared to the explosive research on 2D vdW materials, quasi-one-dimensional (quasi-1D) vdW materials have received rare attention, despite they also present rich physics in electronics and engineering implications. Herein, quasi-1D MoS_2 nanoscrolls are directly fabricated from CVD-grown 2D triangular MoS_2 sheet. The formation, stability and electronic property of quasi-1D MoS_2 nanoscrolls are studied experimentally and theoretically. The formation of nanoscroll always starts from the edge of triangular MoS_2 sheet along its armchair orientation. The electronic properties of MoS_2 nanoscrolls are systemically studied with optical spectroscopy, electrical transport together with density-functional theory (DFT) calculations. Surprisingly, the carrier mobility and contact property of MoS_2 nanoscroll based field effect transistors (FETs) distinct from that of 2D MoS_2 sheet. The transition from 2D semiconductor MoS_2 sheet to 1D metallic MoS_2 nanoscroll is successfully achieved. It is expected that this method of fabricating MoS_2 nanoscrolls will attract wide interest for 1D transition metal dichalcogenides with novel physical and chemical properties.

Introduction

The Beyond graphene, 2D layered vdW materials have been recognized as a basic building block for nanomaterials with all other dimensionalities. For example 2D vdW materials can be wrapped up into 0D, rolled into 1D or stacked into 3D materials.[1-3] With the change of dimensionalities, vdW materials have shown unique properties include tunability of energy structure (from indirect to direct bandgap) and variations of many-body quantum criticalities.[4-7]

As a representative member of vdW family, molybdenum disulfide (MoS_2) displays excellent properties when its dimensionality varies from 0D to 3D. 0D MoS_2 i.e. quantum dots, exhibits special electronic and photo-physical properties due to the quantum confinement and edge effects which enable its application in bio-imaging, luminescent sensing and catalysts.[8-11] While, the high carrier mobility and reasonable bandgap of 2D MoS_2 sheet together with its compatible fabrication make it promising candidate for next diverse electronics in the semiconductor industry.[12, 13] In addition, the 3D MoS_2 bulk materials with small friction coefficient makes its excellent application in lubrication.[14-16] However, 1D MoS_2 has received considerably less attention even it is expect to inherit excellent property.[17] In 2001, 1D MoS_2 nanotube has been first synthesized under ultrahigh temperature with long time by bottom-to-up method, but the poor morphology and quality limited its application.[18, 19] 1D MoS_2 nanoscrolls, as another prototypical structure of 1D MoS_2, is a spirally wrapped 2D MoS_2 sheet.[20] Recently, 1D MoS_2 nanoscroll was prepared by plasma treatment and chemical route, however, the poor morphology, atomic defect and unexpected contamination degrade its quality and further limit its application.[21-24] Up to now, all studies are limited on synthesis. The mechanical strength has been only studied by theoretical simulation,[25] but the electronic property of 1D MoS_2 nanoscrolls from experimental and theoretical investigation has never been reported impeding by the experimental difficulties in fabrication, isolation, and device integration.

In this study, we introduce a simple and efficient method to prepare 1D MoS_2 nanoscroll directly from chemical vapor deposition (CVD) grown 2D MoS_2 sheet at room temperature. Combining the experiments and theory calculations, the formation of 1D MoS_2 nanoscroll is investigated in detail. A major finding from our experiment is that the 2D MoS_2 sheet always scrolls from its Mo-terminated edge with an armchair orientation. Molecular dynamics simulation and DFT computation provide a sensible explanation to this experimental phenomenon. The band structure of 1D MoS_2 nanoscrolls with different layers of wall is computed, illustrating its unique electronic property. In particular, 1D MoS_2 nanoscroll with three-layer wall exhibits metallic-like

[a] Department of Materials Science, Sichuan University, Chengdu 610064, China.
[b] Interdisciplinary Nanoscience Center (iNANO), Aarhus University, DK-8000 Aarhus C, Denmark.
[c] Department of Chemistry, University of Nebraska-Lincoln, NE 68588 Lincoln, United States.
[d] Key Laboratory of Colloid and Interface Chemistry, Ministry of Education, Shandong University, Jinan, 250100, China.
[e] Department of Chemical & Biomolecular Engineering and Department of Mechanical & Materials Engineering, University of Nebraska-Lincoln, NE 68588 Lincoln, United States.

† Electronic Supplementary Information (ESI) available: Experimental Section and Computation Methods, Additional Figs. S1-S8. See DOI: 10.1039/x0xx00000x

‡ These authors contributed equally to this work.

behavior. The spectroscopic properties of 1D MoS_2 nanoscroll have been also measured using X-ray photoemission spectroscopy and Raman microscopy. Importantly, the electronic transport property of 1D MoS_2 nanoscroll is firstly studied, including electric field effect, carrier mobility and contact property, which show a distinct transport behavior from that of 2D MoS_2 sheet.

Results and discussion

Triangular 2D MoS_2 sheet is first grown on SiO_2/Si by CVD, where MoO_3 and sulfur are employed as the sources.[26, 27] Next, 2D MoS_2 sheet is transferred onto a new SiO_2/Si substrate as shown in Fig. 1a. By dropping ~100 μL isopropyl alcohol (IPA) solution on the surface, the adsorption interaction between MoS_2 sheet and substrate is reduced by inserted IPA solution,[28] and then MoS_2 has turned from 2D sheet to quasi-1D nanoscroll structure at room temperature within several minutes. Fig. 1b shows the typical partially scrolled MoS_2 nanoscroll/sheet, and the inset shows the fully scrolled MoS_2 nanoscroll. The length of MoS_2 nanoscroll is defined by the size of 2D MoS_2 sheet itself. The morphology and uniformity is much more perfect than those of previously reported MoS_2 nanoscroll.[21-24] Interestingly, the scrolling directions (black arrow indicated) always keep perpendicular to MoS_2 edge, and the scrolling always starts from its edge rather than corner. This indicates that the scrolling is driven by internal vdW force

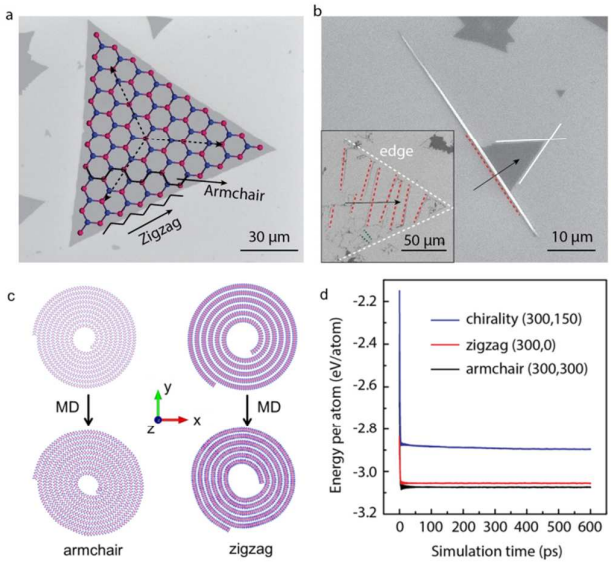

Fig. 1. The formation of MoS_2 nanoscrolls. a) and b) SEM images of MoS_2 sheet and nanoscrolls on SiO_2 substrate. The inset in b) shows the low magnification SEM image. c) The same-sized MoS_2 sheet scrolled via the armchair (left panels) and zigzag (right panels) orientation before (upper panels) and after (lower panels) the structure relaxation at 300 K and 1 bar through classical MD simulation. d) The computed energy per atom of the system versus simulation time for MoS_2 nanoscrolls with armchair, zigzag and chirality (300, 150) orientation, respectively.

rather than external IPA evaporation because the MoS_2 edge is subjected to stronger internal vdW force than the MoS_2 corner. A schematic of MoS_2 atomic model (inset in Fig. 1a) illustrates the Mo-terminated edges of CVD-grown 2D MoS_2 sheet.[29, 30] Thus, it suggests that the scrolling orientation (black arrow indicated in Fig. 1b) is parallel to armchair direction shown the dashed black arrow in Fig. 1b. The as-grown 2D MoS_2 sheet has also been scrolled as shown in Fig. S1, where one can see that a large amount of short and small MoS_2 nanoscrolls are formed. This is caused by the strong interaction between as-grown MoS_2 and SiO_2 substrate, which makes MoS_2 sheet breaks up into many fragments during scrolling. The scrolling orientation is summarized in Fig. S1. Interestingly, the scrolling orientation is also near perpendicular to MoS_2 edge with period about 60°, which indicates that the scrolling orientation is independent to the size of MoS_2 nanoscrolls. To gain molecular-level insight into the dominant tendency for MoS_2 sheet scrolling via the armchair orientation, we performed a classical MD simulation. As shown in Fig. 1c and 1d, the energy per atom for the nanoscroll scrolled via the armchair orientation is lower than that via the zigzag and other chirality (i.e., (300, 150)) orientation, consistent with the experiment.

Moreover, a MD simulation of the self-scrolling process in real time is performed for two-layer MoS_2 sheet with partially scrolled structure as the initial time (0 ps) (see Fig. 2a; more detailed snapshots are displayed in Fig. S2, one more shorter MoS_2 sheet is also investigated as shown in Fig. S3).[31] During the ensuring scrolling, the left portion of MoS_2 sheet moves closer to the nanoscroll at ~ 25 ps, and then begins to wrap onto the existing partial MoS_2 nanoscroll at ~ 100 ps (see Fig. S2). This attaching-wrapping process continues until the whole MoS_2 sheet turns into a full nanoscroll at ~ 200 ps (Supporting Video S1). Fig. 2b presents the energy per atom of the system

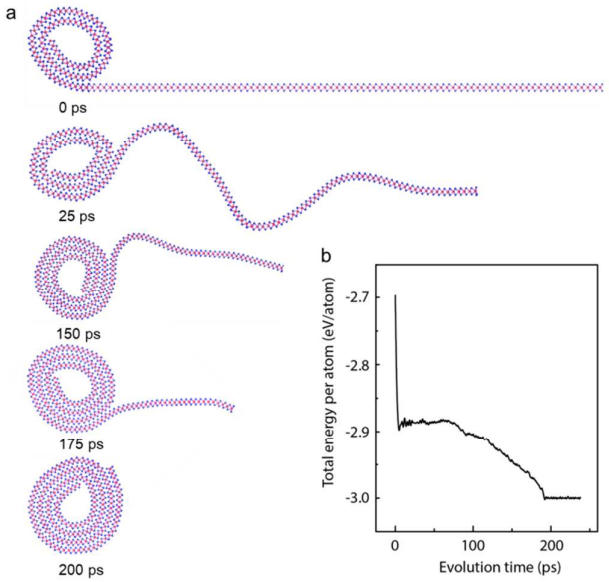

Fig. 2. a) The snapshots of MoS_2 sheet self-scrolling at time 0, 25, 150, 175 and 200 ps; b) the energy of the system versus MD simulation time during the self-scrolling at 300 K.

as a function of time for the self-scrolling process. Clearly, beyond 200 ps the MoS_2 nanoscroll reaches a relatively stable state without showing much energy variation. This MD simulation demonstrates that the self-scrolling process can be a very fast process the formation of the initial partial nanoscrolls.

To see clearer structural details of the fabricated nanoscrolls, MoS_2 nanoscrolls are transferred on grid for high-resolution transmission electron microscope (HR-TEM) characterization. The HR-TEM image (Fig. 3a) shows that it possesses a tube-like structure with a hollow core surrounded by thick walls consisting of MoS_2 multilayer. The HR-TEM image clearly shows the MoS_2 layers are uniformly and compactly stacked. The interlayer distance between adjacent MoS_2 layers is summarized in Fig. 3b (other HRTEM images are shown in Fig. S4), which ranges from 5.5 Å to 6.5 Å, consistent with that of MoS_2 bulk material and MoS_2 nanotubes.[32, 33] Some interlayer distance is as large as 10 nm (Fig. S5), which should be caused by the uncontrollably scrolling speed. In addition, too large size of MoS_2 sheet will also render to form uniformly nanoscrolls due to the non-uniformly strain during scrolling. To confirm the stability of different structures, MD simulation of MoS_2 nanoscroll with interlayer distance ranging from 4 Å to 10 Å are performed as shown in Fig. 3c and 3d. MoS_2 nanoscroll tends to form highly defected structure or collapsed structure if the interlayer distance is smaller than 4.5 Å or larger than 6.5 Å, respectively. If the interlayer distance increases from 4 Å to 10 Å, the energy per atom (Fig. 3d) will decrease from -2.97 eV to -3.07 eV and then increase to -3.01 eV. The energy per atom as a function of interlayer distance clearly demonstrates that the system is at the energetically favourable state when the interlayer distance is within the range from 4.7 to 6.5 Å, consistent with the experimental observation. When the interlayer distance is beyond 7 Å, the collapsed pore structure will be formed, again accordant with the experimental observations (Fig. S5). This is because either smaller or larger interlayer distance can increase either the repulsive or attractive vdW interaction, thereby causing highly defected structure.

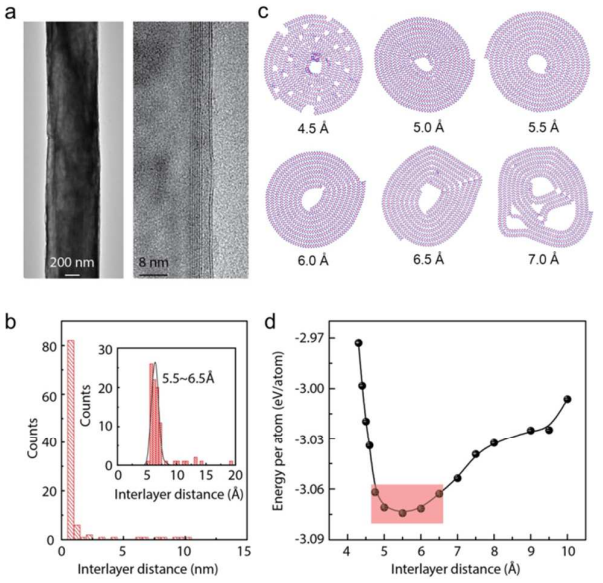

Fig. 3. The stability of MoS_2 nanoscrolls. a) The TEM and HR-TEM images of MoS_2 nanoscroll. b) The histogram of interlayer distance of MoS_2 nanoscrolls, the inset shows the more localized histogram. c) The MD simulation of MoS_2 nanoscrolls with different interlayer distance, ranging from 4.5 Å to 7.0 Å. d) The energy per atom as a function of interlayer distance for the MoS_2 nanoscroll. The red rectangle highlights interlayer distances that give energetically favorable structures with little defects.

Experimentally, Raman and X-ray photoelectron spectroscopies (XPS) are employed to study the optical property and electronic structure of MoS_2 sheet and nanoscroll, as presented in Fig. 4. The high-resolution Mo 3d and S 2p XPS spectra have been carefully calibrated by C1s peak from surface contamination. As shown, the blue shifts (increase in binding energy) are observed in the binding energy of core levels in MoS_2 after scrolling. After scrolling, the binding energy of Mo $3d_{5/2}$ shifts from 229.38 eV to 229.84 eV, whereas the peak of S $2p_{3/2}$ shifts from 162.25 eV to 162.71 eV. Since the Fermi level in material is related to the binding energy,[26, 34] the blue shifts of binding energy can be interpreted by the move up of the Fermi level in MoS_2 nanoscrolls compared to MoS_2 sheet, suggesting a distinct electronic structure in MoS_2 nanoscrolls. Fig. 4b shows the Raman spectra of MoS_2 sheet and nanoscrolls. It is obvious that E_{2g} and A_{1g} bands red and blue shift, respectively. Furthermore, the position difference between A_{1g} and E_{2g} increases from 19.2 cm^{-1} to 22.5 cm^{-1}, indicating a strong interlayer interaction which is similar with that of thick MoS_2.[35]

Because the fabricated MoS_2 nanoscrolls are too large for the first-principles DFT computation, to understand the electronic properties of the nanoscrolls, we computed the band structures of two limiting systems, namely, model multilayered MoS_2 nanosheets and model multi-walled MoS_2 nanotubes (see Fig. S6). Fig. 5a-c show the computed band structure and the corresponding density of states (DOS) for 2D 1 layer (1L)-3 layer (3L) MoS_2 sheet. Clearly, with increasing the number of layers from 1L to 3L, the computed band gap decreases from 1.74 eV to 1.10 eV, a trend consistent with previous results.[36, 37] On the other hand, for the multi-walled MoS_2 armchair nanotubes with the wall-to-wall distance about 5.5 Å, the computed band structure and corresponding DOS for single-, double- and triple-walled MoS_2 nanotube, respectively, are presented in Fig. 5d-e. Notably, the computed

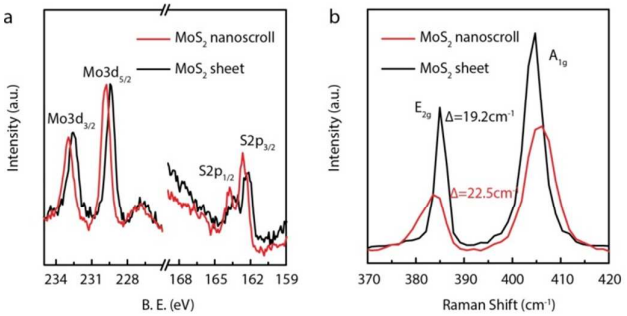

Fig. 4. The spectroscopic characteristic of MoS_2 sheet and nanoscroll. a) the high resolution Mo 3d and S 2p XPS spectra

of MoS_2 sheet and nanoscroll. b) the Raman spectra of MoS_2 sheet and nanoscroll.

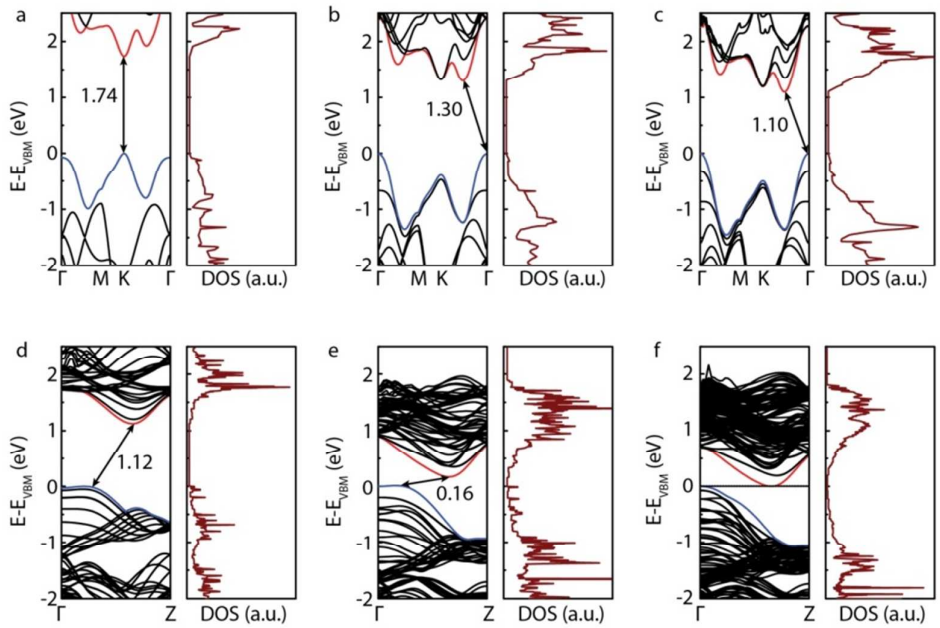

Fig. 5. The band structure of MoS_2 nanostructures. a)-c) The band structure and corresponding DOS distribution of 1L, 2L and 3L MoS_2 nanosheets. d)-f) The band structure and corresponding DOS distribution of MoS_2 nanotube with single-, double- and triple-walled MoS_2 nanotube.

band gap decreases monotonously from 1.12 eV to 0 eV, with thickness increasing from single to triple walled nanotube. In particular, the zero band gap for the triple-walled nanotube indicates that the nanotube already becomes a metal. The two limiting cases indicate that the trend of band-gap change as a function of layer number for 2D MoS_2 sheets is dramatically different from that for 1D MoS_2 nanotubes. The band gap of 2D MoS_2, as tuned by the layer number, is lower bounded by the value 0.88 eV of the bulk MoS_2.[38] On the other hand, the trend of band-gap change for 1D MoS_2 nanoscroll is expected to resemble that of 1D MoS_2 nanotubes. Hence, we expect the semiconductor-to-metal transition (or appearance of zero band gap) would occur for 1D MoS_2 nanoscroll at a layer number greater than three.

To explore the electronic transport property, back-gated field effect transistors (FETs) have been fabricated employing MoS_2 sheet and nanoscroll as the channel materials. Ti (10nm)/Au (50nm) as the drain and source electrodes were defined by electron beam lithography, and deposited by electron beam deposition system followed with lift-off. The output curves of MoS_2 nanoscroll FET under V_{GS} varying from -70 V to 70 V is shown in Fig. 6a, which exhibit linearly current-voltage characteristic suggesting an ohmic contact behavior. The transfer curves of MoS_2 nanoscroll under different V_{DS} (Fig. S7) show a well and stable field effect. To compare, the transfer curves of MoS_2 sheet and nanoscrolls FETs are plotted together in Fig. 6b. As seen, I_{DS} of MoS_2 nanoscroll FET increase with V_{GS} increasing, suggesting that MoS_2 nanoscroll still shows n-type transport characteristic similar with that of MoS_2 sheet FET. However, the current on/off ratio of MoS_2 nanoscroll FET significantly decreases from ~10^4 to ~10^{-1}, indicating a difference transport behavior from MoS_2 sheet, which suggest MoS_2 nanoscroll exhibits metallic property consisted with zero bandgap from DFT calculation. Contrary to thick MoS_2 sheet which has on/off ratio of about 10^4 (Fig. S8), the lower on/off ratio (~10^{-1}) in MoS_2 nanoscrolls device indicates that the difference transport behavior is originated from its unique structure (continually scrolling structure) rather than the increased thickness.

The carrier mobility in MoS_2 nanoscrolls could be calculated by $\mu_{1D} = (L^2/V_{DS}C_{1D})(dV_{DS}/dV_{GS})$, where L is the channel length. C_{1D} is the capacitance for the case of 1D channel material, which could be calculated by $C_{1D} = (2\pi\varepsilon\varepsilon_0 L)/cosh^{-1}((r+t_{ox})/r))$ where ε is the dielectric constant of SiO_2, t_{ox} is the thickness of SiO_2, r and L are the radius and length of the MoS_2 nanoscroll, respectively.[28, 39] In the case of MoS_2 sheet, the carrier mobility could be calculated by $\mu_{2D} = (L/WV_{DS}C_{2D})(dV_{DS}/dV_{GS})$, where W is

Journal Name

ARTICLE

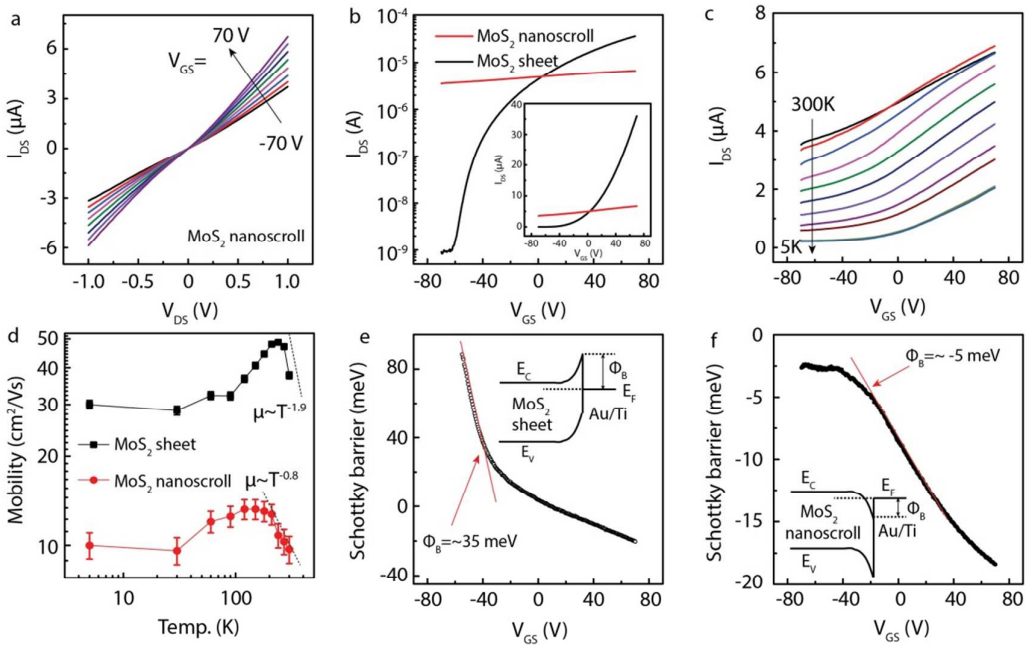

Fig. 6. The electrical transport properties of MoS_2 nanoscrolls. a) The output properties of MoS_2 nanoscroll transistor. b) The transfer curve of MoS_2 sheet and nanoscroll transistors. c) The temperature dependent transfer curves of MoS_2 nanoscroll transistor. d) The mobility as a function of temperature for MoS_2 sheet and nanoscroll. e) and f) The Schottky barrier as a function of gate voltage on MoS_2 sheet and nanoscroll, respectively. The inset shows the corresponded energy diagram structure.

the channel width.[26, 40] C_{2D} is the capacitance for the case of 2D channel material, which could be calculated by $C_{2D} = \varepsilon\varepsilon_0/t_{ox}$. According to the estimation, the carrier mobilities are ~37.5 cm^2/Vs and ~9.7 cm^2/Vs for MoS_2 sheet and nanoscroll, respectively. The smaller mobility of MoS_2 nanoscrolls is resulted from the much weaker capacitance coupled with the back gated compared to that of flat MoS_2 sheet. Even so, the mobility of MoS_2 nanoscroll is much larger than that of MoS_2 nanotube (0.014 cm^2/Vs),[41] possible due to the feature of continuous electron distribution in MoS_2 nanoscrolls. Furthermore, the temperature dependent transfer curves of MoS_2 sheet and nanoscrolls FETs are performed, as shown in Fig. 6c and Fig. S9. The temperature dependent mobilities are plotted in Fig. 6d, where one can clearly see that MoS_2 sheet always has a higher mobility than that of MoS_2 nanoscroll. With temperature cooling, the mobility for MoS_2 sheet and nanoscroll will both increase and then decrease, exhibiting a peak at around ~240 K and ~180K, respectively. This phenomenon is related to the dominated carrier scattering mechanism which change from electron-phonon scattering to charged impurity scattering during cooling.[42] Furthermore, fitting the plot with $\mu \sim T^{-\gamma}$ in electron-phonon dominated part, one can see that the value of γ for MoS_2 sheet is 1.9 which is similar with previous results.[42] Significantly, the value of γ for MoS_2 nanoscroll is 0.8, which is much smaller than that of MoS_2 sheet and bulk MoS_2 ($\gamma = 2.6$).[43, 44] This suggests that the electron-phonon scattering in MoS_2 nanoscroll is weaker than that of MoS_2 sheet even the bulk MoS_2 possibly attributing to its confined structure.

Furthermore, the contact property of MoS_2 nanoscrolls could be studied to explore its energy band structure. To evaluate the Schottky barrier height between metal contact with MoS_2, the temperature dependence of the I_{DS}-V_{GS} curve could be re-plotted with Arrhenius formation with $\ln(I_{DS}/T^{\frac{3}{2}}) \sim 1000/T$, as shown in Fig. S10. As seen, the $\ln(I_{DS}/T^{\frac{3}{2}}) \sim 1000/T$ has positive correlations for MoS_2 nanoscroll compared with negative correlations for MoS_2 sheet in the temperature range from 300 K to 200 K. Furthermore, the effective Schottky barrier could be obtained from the slope of the Arrhenius plot, as summarized in Fig. 6e and 6f. In the case of MoS_2 sheet (Fig. 6e), the Schottky barrier dramatically decreases from ~85 to 0 meV, becomes negative, and finally

saturates near – 20 meV with V_{GS} increase. A sudden change with Schottky barrier of 35 meV is observed which should be due to the dominated mechanism switching from thermionic emission to quantum-mechanical tunnelling when the V_{GS} increase.[45-47] Therefore, it indicates that the effective Schottky barrier is ~ 35 meV for the particular device, as indicating in Fig. 6e. Different to MoS_2 sheet, the Schottky barrier of MoS_2 nanoscrolls slowly decreases from -2.5 meV to -5 meV, and then rapidly decreases to -17 meV when V_{GS} increase. This indicates that the effective Schottky barrier is ~ -5 meV for the particular device, as indicating in Fig. 6f. According to the Schottky-Mott model,[48] the Schottky barrier could be estimated based on the work function of the metal contact (Φ_{metal}) relative to the electron affinity of materials ($\chi_{material}$) by $\Phi_B = \Phi_{metal} - \chi_{material}$. Therefore, the negative Schottky barrier suggests that the affinity of MoS_2 nanoscroll is slightly bigger than the work function of metal contact. With the similar metal contact, it can be concluded that the affinity of MoS_2 nanoscroll is ~ 40 meV bigger than that of MoS_2 sheet with $\Delta\chi_{material} = -\Delta\Phi_B$. The energy diagram inset in Fig. 6e and 6f shows the relative location of energy band, where the energy diagram of MoS_2 nanoscroll is quite different from MoS_2 sheet.[33] Hence, we demonstrate that the transition from semiconductor 2D MoS_2 sheet to metallic quasi-1D MoS_2 nanoscroll by self-rolling method.

Experimental

Experimental Section

Synthesis of MoS_2 sheet: The MoS_2 sheet were grown by the chemical vapor deposition (CVD) method. 500 mg sulfur powder was put at the upstream of the furnace with temperature of ~200 °C. MoO_3 powder was placed in a quartz boat located in the center of the furnace. A SiO_2/Si substrate was facedown placed on top of the quartz boat. The furnace was first purged with 50 sccm Ar for 30 min and kept the furnace pressure in the range of 1-3 kPa during the whole growth process, then raised to the growth temperature 850 °C in 30 min. When the furnace reached 750 °C, the temperature of sulfur reached 200 °C. After growing 10 min, the power for heating furnace was terminated, and the system cooled naturally. When the temperature was lower than 600 °C, the power for heating sulfur was switched off.

Transfer of MoS_2 sheet and prepare MoS_2 nanoscrolls: PMMA layer was formed on the surface of MoS_2/SiO_2/Si by spin-coating. The sample was baked at 180 °C for 5 min, and then put into DI water to release PMMA/MoS_2 from the substrate. After that, a new SiO_2/Si substrate was used to pick up the PMMA/MoS_2. After drying in nature, the PMMA was removed by warm acetone for three times. The sample was then heated at 80 °C for 5 min. To form the MoS_2 nanoscrolls, 100~500 μL isopropyl alcohol (IPA) was carefully dropped on the surface according the size of substrate. When the solution was vapored, the MoS_2 nanoscrolls were formed. It should be noted that there are some parameters which will influence the scrolling process, for example the clean and size of MoS_2 sheet. The remained contaminations will prevent the scrolling due to the difficult inserting of IPA solution. Too large size of MoS_2 sheet will results in un-uniform MoS_2 nanoscrolls possible due to the random defect.

Device fabrication and Characterization: The electrodes were pattered by electron beam lithography. 10 nm Ti/50 nm Au layers were deposited by electron beam deposition with 0.2 Å/s. The source and drain electrodes were formed after lift-off. The electrical property of field effect transistor was measured in vacuum probe station with Keithley 4200 SCS. The Raman spectroscopy measurements were carried out on Renishaw inVia Raman Spectroscope with 514 nm and 1.0 mW laser excitation. The XPS measurements were carried out on Kratos Axis Ultra DLD spectrometer under a vacuum of 1×10^{-9} torr. To prepare the sample for TEM measurement, a PMMA layer was spin-coated on MoS_2 nanoscrolls/SiO_2/Si. After baked at 100 °C for 5 min, PMMA/MoS_2 nanoscrolls/SiO_2/Si was immersed into DI water, and then PMMA/MoS_2 nanoscrolls member would release from SiO_2/Si substrate. The member was picked up by TEM grid and dry in air. The PMMA was removed by warm acetone leaving MoS_2 nanoscrolls on TEM grid.

Computation Methods

We perform all the classical molecular dynamics (MD) simulation by using large-scale atomic/molecular massively parallel simulator (LAMMPS) within the isothermal-isobaric (NPT) ensemble.[49] The Stillinger–Weber (SW) potential developed by Kandemir et al[50] is employed to describe the interatomic interactions of MoS_2 nanoscrolls. The formula of SW potential is divided into a two-body bond stretching term and a three-body bond bending term. To ensure an accurate description of the three-body bond bending term, the top layer S atoms are treated as a different type of atoms from the bottom layer S atoms. Each nanoscroll model is constructed with the axial direction under periodic boundary conditions. Our MD runs consist of at least 1,200,000 time steps with each time step of 0.5 fs. Each run time is at least 600 ps. All the classical MD simulations are conducted at room temperature 300 K. For the density functional theory (DFT) calculations, we adopt the Perdew-Burke-Ernzerhof functional within the general gradient approximation, as implemented in the Vienna ab initio simulation package (VASP 5.4).[51,52] A plane-wave energy cutoff of 500 eV is used. The lattice constants and all atomic positions are fully relaxed by the conjugate gradient procedure until all the atomic forces are less than 0.01 eV. The tolerance for energy convergence is set to 10^5 eV. A Monkhorst–Pack mesh of 12×12×1 and 1×1× 6 *k*-points are used to sample the Brillouin zone of the MoS_2 multi-layered nanosheet and multi-walled nanotube, respectively. The index for the single-, two- and tripled-walled MoS_2 nanotubes are (12, 12), (6, 6)-(12, 12) and (6, 6)-(12, 12)-(18, 18), respectively.

Conclusions

In summary, the MoS_2 nanoscrolls are fabricated from CVD-grown MoS_2 sheet successfully. The formation of nanoscrolls always starts from triangular MoS_2 edge and the scrolling direction is perpendicular to MoS_2 edge along armchair direction, which suggests scrolling is driven by the internal

vdW interaction. Classical MD simulation is applied to investigate the dynamic formation of MoS_2 nanoscroll. Furthermore, the band structure of MoS_2 nanosheets and nanotubes, tow limiting dimensional systems for the nanoscrolls, is calculated by DFT method. The electronic structure is also discussed base on its optical spectroscopies. According to the electronic transport property from low temperature electrical measurement, the carrier mobility and Schottky barrier are systematically investigated. In contrary to semiconducting 2D MoS_2 sheet, the quasi-1D MoS_2 nanoscroll shows a metallic-like behavior with low current on/off ratio, higher carrier mobility, negative Schottky barrier, possibly due to its notable feature of continues electron distribution and strong electron-electron interaction. Such self-scrolling method can be easily applied to fabricate other 1D TMDs with unique functionality and extend potential application of TMDs.

Conflicts of interest

There are no conflicts to declare.

Acknowledgements

This research was supported by grants from the Danish National Research Foundation, AUFF-NOVA project from Aarhus Universitets Forskningsfond, EU H2020RISE 2016-MNR4S Cell project. X.C.Z. was supported by US NSF through the Nebraska Materials Research Science and Engineering Center (MRSEC) (grant No. DMR-1420645) and by UNL Holland Computing Center.

Notes and references

1 A. K. Geim and K. S. Novoselov, *Nat. Mater.*, 2007, **6**, 183.
2 Z. Wang, Q. Li, H. Xu, C. Dahl-Petesen, Q. Yang, D. Cheng, D. Cao, F. Besenbacher, J. V. Lauritsen, S. Helveg, M. Dong, *Nano Energy*, 2018, **49**, 634.
3 D. Jariwala, T. J. Marks and M. C. Hersam, *Nat. Mater.*, 2016, **16**, 170.
4 M. Bonilla, S. Kolekar, Y. Ma, H. C. Diaz, V. Kalappattil, R. Das, T. Eggers, H. R. Gutierrez, M.-H. Phan and M. Batzill, *Nat. Nanotech.*, 2018, DOI: 10.1038/s41565-018-0063-9.
5 Y. Liu, N. O. Weiss, X. Duan, H.-C. Cheng, Y. Huang and X. Duan, *Nat. Rev. Mater.*, 2016, **1**, 16042.
6 Z. Wang, Q. Li, Y. Chen, B. Cui, Y. Li, F. Besenbacher and M. Dong, *NPG Asia Mater.*, 2018, doi.org/10.1038/s41427-018-0062-1.
7 A. Zhang and C. M. Lieber, *Chem. Rev.*, 2016, **116**, 215.
8 S. Xu, D. Li and P. Wu, *Adv. Funct. Mater.*, 2015, **25**, 1127.
9 B. Mohanty, M. Ghorbani-Asl, S. Kretschmer, A. Ghosh, P. Guha, S. K. Panda, B. Jena, A. V. Krasheninnikov and B. K. Jena, *ACS Catal.*, 2018, **8**, 1683.
10 C. Tan, Z. Luo, A. Chaturvedi, Y. Cai, Y. Du, Y. Gong, Y. Huang, Z. Lai, X. Zhang, L. Zheng, X. Qi, M. H. Goh, J. Wang, S. Han, X.-J. Wu, L. Gu, C. Kloc and H. Zhang, *Adv. Mater.*, 2018, DOI: 10.1002/adma.201705509.
11 K. Zhou, Y. Zhang, Z. Xia and W. Wei, *Nanotechnology*, 2016, **27**, 275101.
12 K. Kang, S. Xie, L. Huang, Y. Han, P. Y. Huang, K. F. Mak, C.-J. Kim, D. Muller and J. Park, *Nature*, 2015, **520**, 656.
13 R. Cheng, S. Jiang, Y. Chen, Y. Liu, N. Weiss, H.-C. Cheng, H. Wu, Y. Huang and X. Duan, *Nature Commun.*, 2014, **5**, 5143.
14 M. Chhowalla and G. A. J. Amaratunga, *Nature*, 2000, **407**, 164.
15 W. O. Winer, *Wear*, 1967, **10**, 422.
16 C. Lee, Q. Li, W. Kalb, X.-Z. Liu, H. Berger, R. W. Carpick and J. Hone, *Science*, 2010, **328**, 76.
17 R. W. Day, M. N. Mankin and C. M. Lieber, *Nano Lett.*, 2016, **16**, 2830.
18 M. Remskar, A. Mrzel, Z. Skraba, A. Jesih, M. Ceh, J. Demšar, P. Stadelmann, F. Lévy and D. Mihailovic, *Science*, 2001, **292**, 479.
19 M. Nath, A. Govindaraj and C. N. R. Rao, *Adv. Mater.*, 2001, **13**, 283.
20 Z. Xu, B. Zheng, J. Chen and C. Gao, *Chem. Mater.*, 2014, **26**, 6811.
21 J. Meng, G. Wang, X. Li, X. Lu, J. Zhang, H. Yu, W. Chen, L. Du, M. Liao, J. Zhao, P. Chen, J. Zhu, X. Bai, D. Shi and G. Zhang, *Small*, 2016, **12**, 3770.
22 X. S. Chu, D. O. Li, A. A. Green and Q. H. Wang, *J. Mater. Chem. C*, 2017, **5**, 11301.
23 P. Thangasamy and M. Sathish, *J. Mater. Chem. C*, 2016, **4**, 1165.
24 D. Y. Hwang, K. H. Choi, J. E. Park and D. H. Suh, *Nanoscale*, 2017, **9**, 503.
25 Z. Liu, J. Gao, G. Zhang, Y. Cheng and Y. Zhang, *Nanotechnology*, 2017, **28**, 385704.
26 Z. Wang, Q. Li, F. Besenbacher and M. Dong, *Adv. Mater.*, 2016, **28**, 10224.
27 X. Yang, Q. Li, G. Hu, Z. Wang, Z. Yang, X. Liu, M. Dong and C. Pan, *Sci. China Mater.*, 2016, **59**, 182.
28 X. Xie, L. Ju, X. Feng, Y. Sun, R. Zhou, K. Liu, S. Fan, Q. Li and K. Jiang, *Nano Lett.*, 2009, **9**, 2565.
29 D. Zhu, H. Shu, F. Jiang, D. Lv, V. Asokan, O. Omar, J. Yuan, Z. Zhang and C. Jin, *NPJ 2D Mater. Appl.*, 2017, **1**, 8.
30 W. Zhou, X. Zou, S. Najmaei, Z. Liu, Y. Shi, J. Kong, J. Lou, P. M. Ajayan, B. I. Yakobson and J.-C. Idrobo, *Nano Lett.*, 2013, **13**, 2615.
31 D. Xia, Q. Xue, J. Xie, H. Chen, C. Lv, F. Besenbacher and M. Dong, *Small*, 2010, **6**, 2010.
32 Y. Zhan, Z. Liu, S. Najmaei, P. M. Ajayan and J. Lou, *Small*, 2012, **8**, 966.
33 S. Fathipour, M. Remskar, A. Varlec, A. Ajoy, R. Yan, S. Vishwanath, S. Rouvimov, W. S. Hwang, H. G. Xing, D. Jena and A. Seabaugh, *Appl. Phys. Lett.*, 2015, **106**, 022114.
34 Y. Chen, S. Huang, X. Ji, K. Adepalli, K. Yin, X. Ling, X. Wang, J. Xue, M. Dresselhaus, J. Kong and B. Yildiz, *ACS Nano*, 2018, DOI: 10.1021/acsnano.7b08418.
35 K.-K. Liu, W. Zhang, Y.-H. Lee, Y.-C. Lin, M.-T. Chang, C.-Y. Su, C.-S. Chang, H. Li, Y. Shi, H. Zhang, C.-S. Lai and L.-J. Li, *Nano Lett.*, 2012, **12**, 1538.
36 K. F. Mak, C. Lee, J. Hone, J. Shan and T. F. Heinz, *Phys. Rev. Lett.*, 2010, **105**, 136805.
37 A. Splendiani, L. Sun, Y. Zhang, T. Li, J. Kim, C.-Y. Chim, G. Galli and F. Wang, *Nano Lett.*, 2010, **10**, 1271.
38 O. V. Yazyev and A. Kis, *Mater. Today*, 2015, **18**, 20.
39 A. C. Ford, J. C. Ho, Y.-L. Chueh, Y.-C. Tseng, Z. Fan, J. Guo, J. Bokor and A. Javey, *Nano Lett.*, 2009, **9**, 360.
40 Z. Wang, P. Li, Y. Chen, J. Liu, W. Zhang, Z. Guo, M. Dong and Y. Li, *J. Mater. Chem. C*, 2015, **3**, 6301.
41 M. Strojnik, A. Kovic, A. Mrzel, J. Buh, J. Strle and D. Mihailovic, *AIP Advances*, 2014, **4**, 097114.
42 B. Radisavljevic and A. Kis, *Nat. Mater.*, 2013, **12**, 815.
43 R. Fivaz and E. Mooser, *Phys. Rev.*, 1967, **163**, 743.
44 D. Yuchen, T. N. Adam, Z. Hong and D. Y. Peide, *J. Phys. Cond. Matter*, 2016, **28**, 263002.
45 D. Qiu and E. K. Kim, *Sci. Rep.*, 2015, **5**, 13743.

46 W. Wang, Y. Liu, L. Tang, Y. Jin, T. Zhao and F. Xiu, *Sci. Rep.*, 2014, **4**, 6928.
47 W. L. Chow, P. Yu, F. Liu, J. Hong, X. Wang, Q. Zeng, C.-H. Hsu, C. Zhu, J. Zhou, X. Wang, J. Xia, J. Yan, Y. Chen, D. Wu, T. Yu, Z. Shen, H. Lin, C. Jin, B. K. Tay and Z. Liu, *Adv. Mater.*, 2017, **29**, 1602969-n/a.
48 S. M. Sze, Ng, K. K., *John Wiley & Sons*, 2006.
49 S. Plimpton, *J. Comput. Phys.*, 1995, **117**, 1.
50 K. Ali, Y. Haluk, K. Alper, Ç. Tahir and S. Cem, *Nanotechnology*, 2016, 27, 055703.
51 G. Kresse and J. Furthmüller, *Phys. Rev. B* 1996, **54**, 11169.
52 H.-H. Wu, Q. Meng, H. Huang, C. T. Liu and X.-L. Wang, *Phys. Chem. Chem. Phys.* 2018, **20**, 3608.

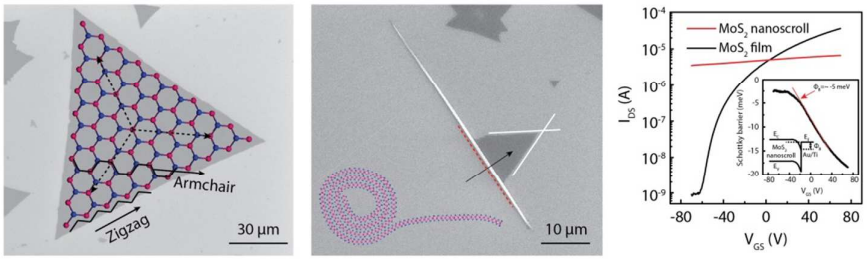

Herein, the properties of quasi-1D MoS_2 nanoscrolls are systemically studied via experiment and theoretical simulation demonstrating that MoS_2 can transmit from semiconductor to metallic by self-scrolling.